

Influence of Nanocrystalline ZrO₂ Additives on the Fracture Toughness and Hardness of Spark Plasma Activated Sintered WC/ZrO₂ Nanocomposites Obtained by Mechanical Mixing Method

M. Sherif El-Eskandarany¹, Hesham M. A. Soliman², M. Omoric³

¹Mining, Metallurgy and Petroleum Engineering Department, Faculty of Engineering, Al Azhar University, Cairo, Egypt; ²Advanced Technology and New Materials Research Institute, City for Scientific Research and Technology Applications, Alexandria, Egypt; ³Institute for Materials Research, Tohoku University, Miyagi, Japan.

Email: h.soliman@mucsat.sci.eg

Received October 11th, 2011; revised November 18th, 2011; accepted December 16, 2011.

ABSTRACT

The present study reports the formation of ultrafine hard particles of nanocomposite WC with different additions of ZrO₂ powders (0.5 - 20 vol.%). The initial mixed powders of WC with the desired ZrO₂ concentrations were mechanically mixed for 360 ks (end-product) under argon gas atmosphere at room temperature, using high energy ball mill. The end-product consists of average grain size of about 17 nm in diameter. The obtained nanocomposite powders were consolidated into fully dense compact, using spark plasma sintering (SPS) technique in vacuum. The experimental results revealed that the consolidation step, which was conducted at 1673 K with uniaxial pressure ranging from 19.6 to 38.2 MPa for short time (0.18 ks), does not lead to dramatic grain growth in the powders so that the consolidated nanocomposite bulk objects maintain their nanocrystalline behavior, being fine grains with an average size of 63 nm in diameter. The relative densities of consolidated nanocomposite WC/ZrO₂ materials increase from 99.1% for WC-0.5% ZrO₂ to 99.93% for WC-20% ZrO₂. The indentation fracture toughness of the composites can be tailored between 7.31 and 19.46 MPa/m^{1/2} by controlling the volume fraction of ZrO₂ matrix from 0.5% to 20%. The results show that the Poisson's ratio increased monotonically with increasing the ZrO₂ concentrations to get a maximum value of 0.268 for WC-20% ZrO₂. In the whole range of ZrO₂ concentrations (0.5 - 20 vol.%), high hardness values (20.73 to 22.83 GPa) were achieved. The Young's modulus tends to decrease with increasing the volume fraction of the ZrO₂ matrix to reach a minimum value of 583.2 GPa for WC-20% ZrO₂. These hard and tough WC/ZrO₂ nanocomposites are proposed to be employed as higher abrasive-wear resistant materials.

Keywords: Nanocomposite; Tungsten Carbide; Zirconia; Spark Plasma Sintering; Powder Metallurgy; Mechanical Alloying; Microstructure; SEM, HRTEM

1. Introduction

Nanotechnology is an umbrella term for a wide range of technologies concerned with structures and processes of materials that have nanometer scale. Nanocomposites are one of those advanced materials that received much attention due to their unique and unusual properties that proposing them as promising candidates for several structural and wear resistance applications [1]. Nanocomposite materials are formed by dispersing nanocrystalline reinforcement ceramics into metallic matrix, leading to significant improvement in the mechanical and physical properties. It has been reported that both strength and fracture toughness are increased by the order of two to four times than conventional composite materials [2]. Among the transition-

metal carbides, WC has excellent high temperature strength and good corrosion resistance. It shows extremely high hardness value and possesses high values of Young's modulus [3]. Due to its poor fracture toughness and the difficulties in powders consolidation to obtain fully dense compacts, WC is usually mixed with metallic binders, such as Co, Fe, and Ni to form so-called cemented carbides. WC-Co cements with different Co volume fractions ranging from 4% to 14% have been widely used for cutting tools and wear resistant materials. Mechanical mixing method, using ball milling of the reinforcement materials (WC) with several concentrations of Co (metallic matrix) shows significant advantage to obtain nanocomposite WC-Co powders [4,5]. The powders were then consolidated into bulk

objects, using hot pressing technique. The hot-pressed WC-Co powders show remarkable increase in the fracture toughness; however the existence of the metallic binding material leads to a decrease in the hardness and elastic module values. WC-Co cements have some industrial limitations because of the presence of metallic Co matrix (binder) leads to failure at high temperature due to softening. Many efforts have been carried out to achieve superior hardness and toughness combinations through replacing the metallic Co by different types of ceramic nanocrystalline materials to form ceramic matrices (WC nanocomposites) [6-8].

The present work has been addressed in order to study the influence of nanocrystalline ZrO₂ additives on improving the fracture toughness and Poisson's ratio of mechanically mixed WC-ZrO₂ nanocomposites. The selection of ZrO₂ comes from the fact that it has a high thermal stability and excellent mechanical properties such as high bending strength and excellent fracture toughness. We are also proposing a powerful tool for obtaining fully dense nano-ceramic composites, using spark plasma sintering (SPS) technique for the mechanically mixed ceramic powders of WC-ZrO₂.

2. Experimental

In the present study, elemental powders of WC (99.5%, 30 μm) were mixed with different selected volume fractions of ZrO₂ (2% Y₂O₃) powders (99.5%, 10 μm) of 0.5, 5, 10, 15 and 20 vol.%. The mixed powders of each ZrO₂ concentration were sealed in a cylindrical WC vial (250 ml in volume) together with fifty WC balls (10 mm in diameter) in a glove box under argon gas atmosphere. The ball-to-powder weight ratio was maintained at the level of 10:1. The ball-milling experiments were carried out at room temperature, using Fritsch P5 high-energy ball mill at a rotation speed of 250 rpm. The milling experiments were interrupted at regular intervals and small amounts of the milled powders were taken out from the vial in the glove box. The powders were characterized by means of X-ray diffraction (XRD) with CuKα radiation, scanning electron microscope (SEM), transmission electron microscope (TEM) using 200 kV and/or high-resolution transmission electron microscopes (HRTEM).

The end product of the ball-milled nanocomposite powders (after 360 ks) at different ZrO₂ concentrations were individually consolidated into bulk samples, using spark plasma sintering (SPS) method. The consolidation procedure took place in vacuum at 1673 K with a pressure of 19.6 to 38.2 MPa. In order to avoid any undesired grain growth, the sintering process was applied for only 0.18 ks without adding any binding materials. The densities of consolidated WC/ZrO₂ materials were determined by Archimedes' principle, using water immersion method. Vickers indenter with a load of 50 kg was employed to deter-

mine the hardness of the compacted samples. The size of the indentation cracks has been used to determine the fracture toughness (K_{Ic}) of the sample [9]. The hardness and K_{Ic} values reported below are averaged from at least ten indentations. The elastic properties of the bulk samples were determined by nondestructive test using pulse-echo overlap ultrasonic technique using ultrasonic detector.

3. Results and Discussions

XRD technique was employed to follow the structural changes that may occur during ball milling of hcp-WC with different volume fractions t-ZrO₂ powders and after the consolidation process that was achieved at 1673 K, using SPS technique. **Figure 1(a)** displays the XRD pattern of ball milled WC-10% ZrO₂ powders after 43 ks of the milling time. The powders at this early stage of milling still consist of coarse grains, indicated by the existence of sharp Bragg-peaks which are corresponding to the matrix and reinforcement materials of t-ZrO₂ and hcp-WC, respectively. Contrary, the XRD pattern of the final-product **Figure 1(b)**, which was obtained after longer milling time (360 ks), shows a significant broadening in the Bragg lines for both ZrO₂ and WC materials, suggesting the formation of nanocomposite WC-ZrO₂. **Figure 1(c)** depicts the

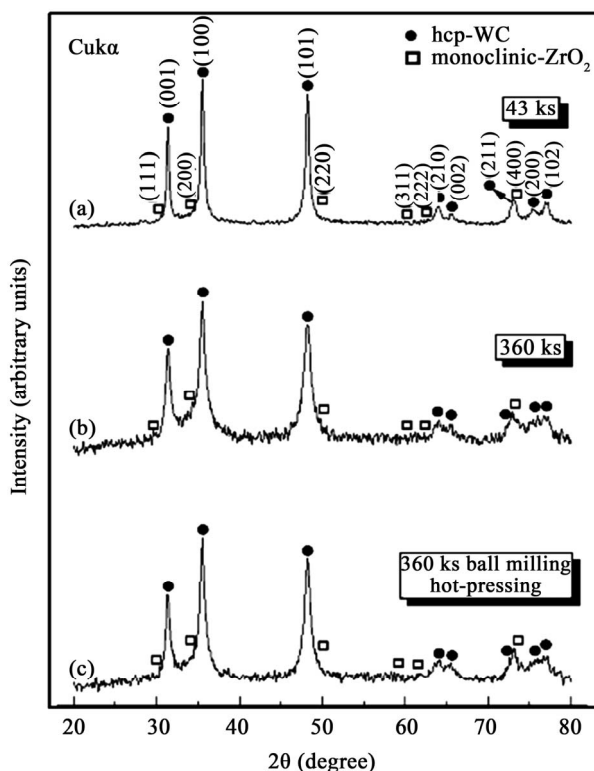


Figure 1. XRD patterns of nanocomposite WC-10 vol.% ZrO₂ after ball milling for (a) 43 ks; (b) 360 ks; (c) for the consolidated sample after ball milling for 360 ks of the final product.

XRD pattern of the final-product (360 ks) that was consolidated at 1673 K indicates the absence of any intermediate phase (s) other than WC and ZrO₂. The absence of any reacted phases during this sintering step implies the thermodynamic compatibility of WC and ZrO₂ at the applied consolidation temperature. Furthermore, there is no obvious dramatic change in the grain size of both the matrix and reinforcement materials can be detected after sintering, indicating that the consolidated sample maintains its nanocrystalline properties (**Figure 1(c)**).

Figure 2 shows the bright field image (BFI) of WC-10% ZrO₂ powders after ball milling for 43 ks (**Figure 2(a)**) and 360 ks (**Figure 2(b)**). The light gray region in **Figure 2(a)** shows the ZrO₂ matrix, whereas the dark coarse grains embedded into the matrix, present the WC grains. The WC grains that are heterogeneously distributed in the matrix have irregular shapes with a wide grain size distribution, ranging from 23 to 280 nm in diameter (**Figure 2(a)**). Obviously, the matrix material at this early stage of milling (43 ks) is either rich or poor with WC. Increasing the milling time (360 ks) leads to successive increase in the impact and shear forces that are generated by the grinding tools (balls) so that the brittle WC grains disintegrated into finer cells with an average diameter of 18 nm in diameter as shown in **Figure 2(b)**. This dramatic disintegration causes an increase in the WC surface area, leading to the formation of nanocrystalline spherical lenses of WC, which are fairly distributed into the whole matrix material to form a homogeneous WC/ZrO₂ nanocomposite. The formation of these nanomaterials is attributed to the plastic deformation that is produced in the WC crystal lattice during the high-energy ball milling process and this occurs by slip and twinning in the lattice of the milled powders. Due to the successive accumulations of the dislocations density, the crystals are disintegrated into sub-grains that are initially separated by low angle grain boundaries. The formation of these sub grains is attributed to the decrease in the atomic level strain. Increasing the ball milling time from 43 ks to 360 ks leads to further lattice distortion and consequently to grain size reduction. Reduction in grain size is very important factor for the consolidation procedure because it increases the sinterability of the powders.

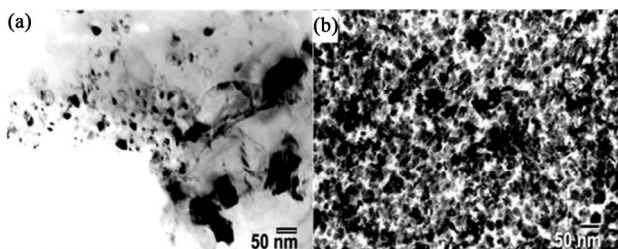


Figure 2. BFI of the ball milled WC-10 vol.% ZrO₂ after milling for (a) 43 ks; (b) 360 ks.

Figure 3 presents the outer macroscopic view of as consolidated samples of WC-10% ZrO₂ (**Figure 3(a-i)**) and WC-20 % ZrO₂ (**Figure 3(a-ii)**) that were obtained after consolidation the powders of the end-product at 1673 K, using SPS technique. The consolidated mirror-like buttons have excellent macroscopic characteristics with the absence of any crack or macro pores (**Figure 3(a)**). To ensure the homogeneity and the vertical density variation of the compacted samples along their longitudinal section, the consolidated button of WC-10% ZrO₂ (**Figure 3(b-i)**) was sectioned into 4 slices with about 20 mm in height for each (**Figure 3(b-ii)**) and the density of each slice was individually measured. However, the highest bulk and relative densities are obtained at the top of this compact; the results do not imply any serious values fluctuations through the longitudinal of the sample, as depicted in **Figure 4(a)**. The variation in the measured relative density of this sample does not exceed above 0.55% (**Figure 4(b)**) suggests the absence of large numbers of pores and also may elucidate the excellent distributions of the WC throughout the whole compact.

The BFI of as-consolidated WC-10% ZrO₂ sample is shown in **Figure 5**. The ZrO₂ matrix (light gray region) consists of equi-axed grains with less than 40 nm in diameter. Likewise the matrix materials, the WC grains (dark grains) were affected by this consolidation step, which leads to a slight grain growth and the formation of edged-like WC grains with a grain size distribution ranging from 20 nm up to 60 nm in diameter (**Figure 5**). It is worth notifying that the WC grains are distributed at the grain boundaries of ZrO₂, however some WC grains tend to agglomerate together in some regions. Thus, we can conclude that WC grains are perfectly interfacial bonded with the ZrO₂ ceramics matrix to form full-dense nanocomposite WC/ZrO₂ material.

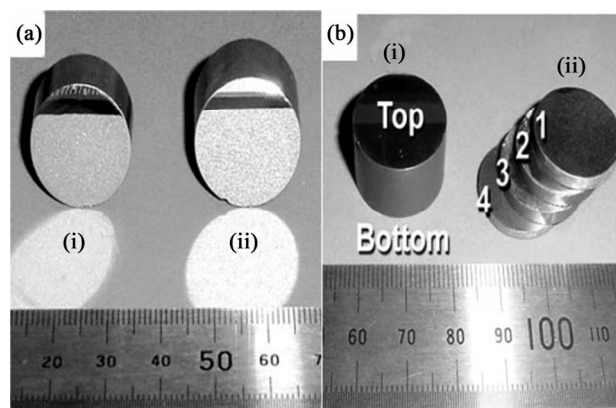


Figure 3. (a) The outer shape of nanocomposite WC mixed with (i) 10 vol.%; (ii) 20 vol.% ZrO₂; (b) Another view of WC-10 vol.% ZrO₂ as one piece (i); as four slices to be used in density measurements (ii).

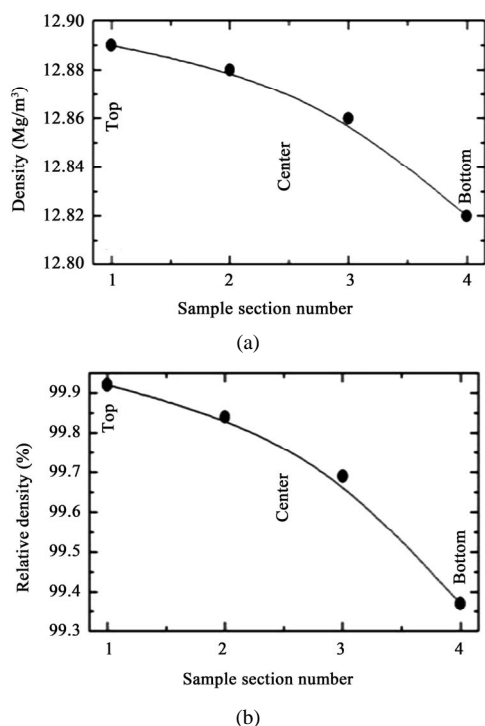


Figure 4. The bulk (a) and relative (b) densities for the sliced sample of WC-10 vol.% ZrO₂.

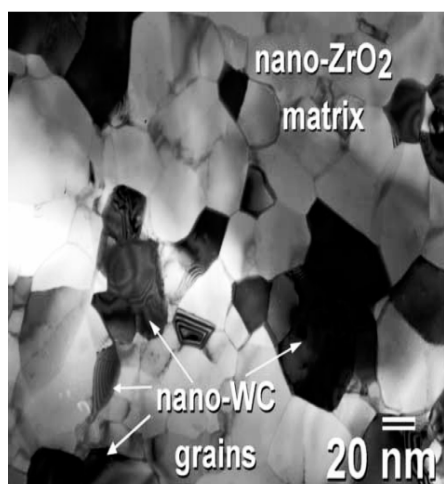


Figure 5. BFI planner view of the end-product of nano-composite WC-10 vol.% ZrO₂ after consolidation.

Further microscopic information was obtained by SEM examinations. The micrograph of the back scattering electron microscope and the elemental dot mapping for W and Zr of the consolidated WC-10% ZrO₂ compact are shown together in **Figure 6**. Obviously, the WC particles that have sharp edges (**Figure 6(a)**) are embedded and homogeneously distributed along the ZrO₂ matrix. Apparently, neither voids nor cracks can be detected, indicating an excellent interfacial bonding. Moreover, no undesirable byproduct could be identified, as suggested by the segregation of the

elemental W and Zr in the composite material on a micron scale (**Figures 6(b)** and **(c)**).

We should emphasize that in the SPS process, several factors contribute to enhance the densification; 1) the use of rapid heating rate of heating and cooling (~600 K/s), 2) rapid transfer of heat because the WC die acts by it- self as a heating element and 3) the application of pulsed DC current to heat the sample, implying that samples are also exposed to a pulsed electric field during the consolidation process. It is believed that application of mechanical pressure promotes the removal of pores and enhances diffusion [10]. However, it is frequently argued the improved densification rates stem mostly from the use of pulsed DC current of high energy. When pulse voltage is applied to the powders, micro-discharge takes place among the particles, which generates plasma. Thus the atoms on the surface of each particle are activated, leading to high sintered densities in very short time. In addition to the application of the pulse electric current that leads to thermal and electric field diffusions within a short time, one important factor is the grain size of the prepared composite powders. The small grain size of the ball-milled powders is considered as important reason for enhancing the driving force during SPS consolidation in that ultrafine particles with their large surface area would be greater inter-particle contact (number of necks) and, hence, more paths for volume diffusion can be achieved [11].

The bulk densities of as-consolidated nanocomposites WC/ZrO₂ materials were measured and plotted in **Figure 7(a)** as a function of ZrO₂ concentrations. Two mathematical expressions were used to predict the effect of ZrO₂ on the density of the composites and to compare the measured values with the theoretical ones. The theoretical density values for different volume fractions were calculated from the rules of mixture, using the upper bound and lower bound equations, that is respectively presented by

$$\rho_{WC-ZrO_2} = \rho_{WC}V_{WC} + \rho_{ZrO_2}V_{ZrO_2}$$

and

$$\rho_{WC-ZrO_2} = \frac{\rho_{WC}\rho_{ZrO_2}}{V_{WC}\rho_{ZrO_2} + V_{ZrO_2}\rho_{WC}}$$

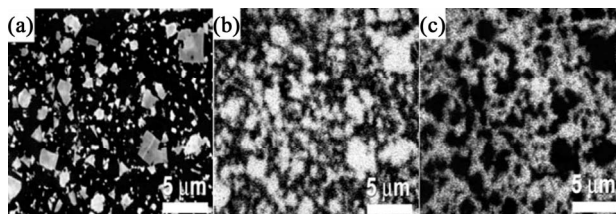


Figure 6. Back scattering view (a) and the dot mapping of elemental W (b) and Zr (c) of nanocomposite WC-10 vol.% ZrO₂ after consolidation.

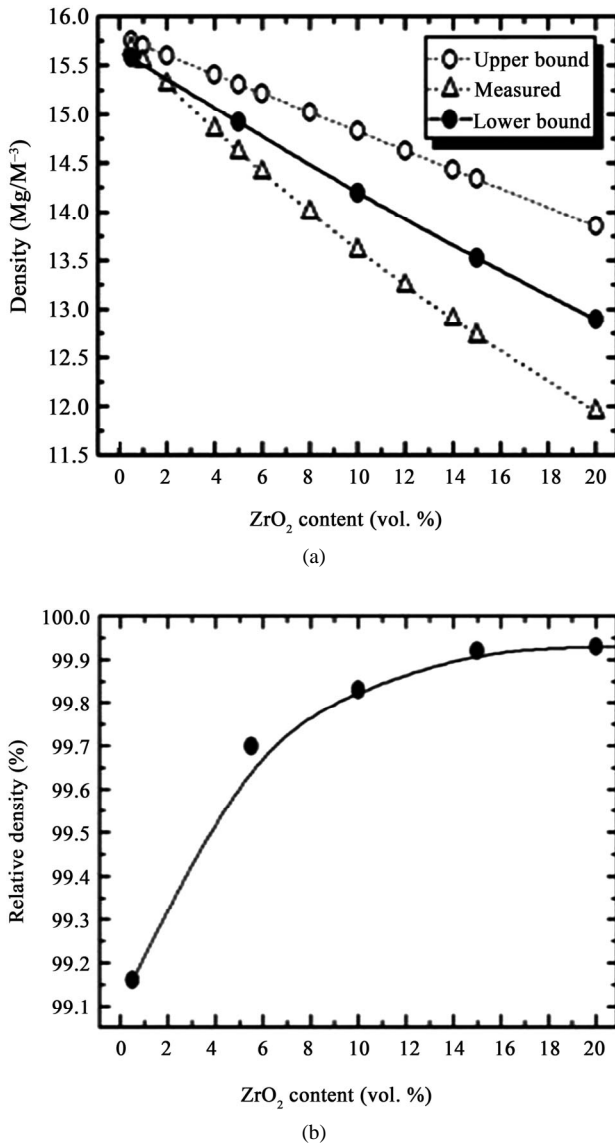


Figure 7. (a) The calculated/theoretical (open symbols) and measured densities (closed symbols) of WC mixed with different ZrO₂ contents; (b) The dependence of the relative density of WC/ZrO₂ on the ZrO₂ contents.

where, ρ and V refer to the density and the volume fraction, respectively. It can be seen that the measured density values of WC/ZrO₂ composites fall between the upper and lower curves, indicating a good matching between the calculated and measured density. The values of the measured density for WC mixed with different ZrO₂ contents are listed in **Table 1**. The correlation between the relative densities of the WC/ZrO₂ composites were calculated and presented in **Figure 7(b)** as a function of ZrO₂ content. All the consolidated samples have relative densities higher than 99.1%, indicating that WC/ZrO₂ nanocomposites can be fully densified at 1673 K, using SPS technique. It can be inferred from the figure that increasing the volume fraction of the matrix material leads to a monotonical increase in the relative density of the composites. This may suggest a monotonical decreasing in the pores and a good bonding between the matrix and reinforcement materials.

A SEM micrograph of the Vickers hardness indentation for consolidated WC-15% ZrO₂ button is shown in **Figure 8**. The hardness of this compact sample was measured and found to be 21.13 GPa, taking the average of at least ten indentations. It is worth noticing that this value is higher than that of bonded nanocomposite WC-14% Co (13.2 GPa) [4]. The measured hardness values of the other WC/ZrO₂ nanocomposites, which are listed in **Table 1** were plotted in **Figure 9** against the ZrO₂ contents (closed symbols). WC/ZrO₂ nanocomposites possess high hardness values (higher than 20.50 GPa) however, the hardness tends to decrease slightly with increasing the soft phase of ZrO₂ content. Going back to **Figure 8**, where the demonstrated cracks in the micrograph were developed in the product during the indentation and extended to 235 μm away from it. These values for different ZrO₂ contents that were used as indicator for estimating the fracture toughness (K_{Ic}) via the model that was proposed by Anstis *et al.* [10] are listed in **Table 1** and plotted in **Figure 9** (open symbols) as a function of ZrO₂ contents. One can say that increasing the ZrO₂ contents improve greatly the fracture toughness

Table 1. Some measured physical and mechanical properties of nanocomposite WC/ZrO₂ with different ZrO₂ concentrations, x.

| Young's Modulus (GPa) | Poisson's Ratio | Modulus of toughness, K_{Ic} (MPa/m ^{1/2}) | Vicker's Hardness (GPa) | Density (Mg-m ⁻³) | X (vol.%) |
|-----------------------|-----------------|--|-------------------------|-------------------------------|-----------|
| 688.2 | 0.008 | 7.31 | 22.83 | 15.580 | 0.5 |
| 641.8 | 0.153 | 9.73 | 22.53 | 14.918 | 5.0 |
| 629.3 | 0.203 | 13.36 | 21.86 | 14.190 | 10.0 |
| 608.1 | 0.251 | 16.83 | 21.13 | 13.520 | 15.0 |
| 583.2 | 0.268 | 19.46 | 20.73 | 12.890 | 20.0 |

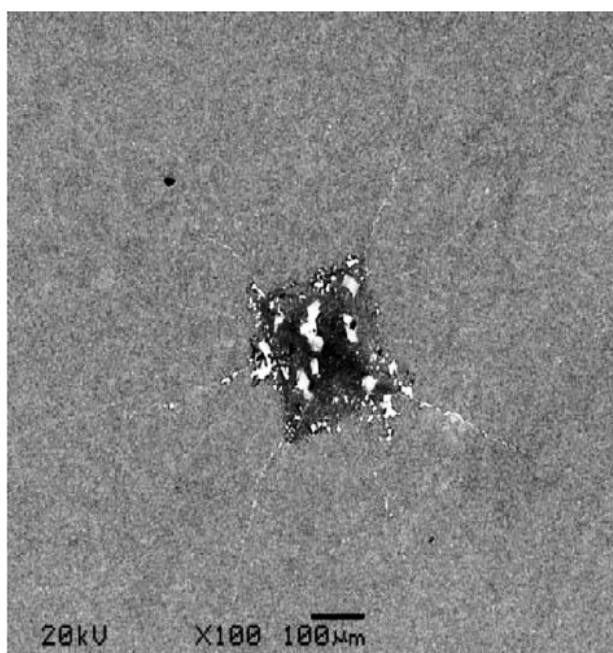


Figure 8. SEM micrograph of Vickers hardness indentation developed by applying a load of 50 kg on the consolidated sample of nanocomposite WC-15 vol.% ZrO₂.

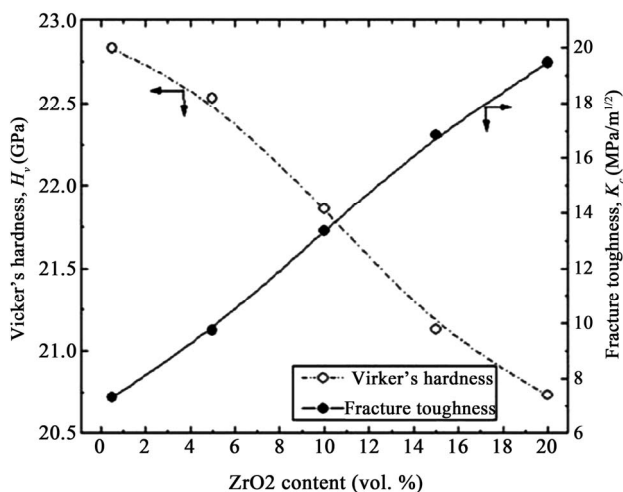


Figure 9. Correlations between Vicker's hardness (open symbols) and fracture toughness (closed symbols) on the ZrO₂ content of nanocomposite WC/ZrO₂.

and a maximum K_c of 19.46 MPa/m^{1/2} was achieved for the composite with 20% ZrO₂ characteristics of the obtained WC/ZrO₂ nanocomposites, indicated by the monotonical increasing in the K_c with increase the ZrO₂ contents. The addition of ZrO₂ increases the fracture toughness due to so-called transformation toughening [13,14]. It is believed that the polymorphic tetragonal-monoclinic phase transformation that takes place in ZrO₂ leads to finite amount of volume change (4% - 5%) and a large shear strain (14% - 15%) [14]. It has been suggested by

Miyazaki *et al.* [12] that the improvement in fracture toughness of the powder- mixture composites is attributed mainly to the "stress-induced" transformation of the ZrO₂ phase.

Figure 10 shows the dependence of the Poisson's ratio (closed symbols) and Young's modulus (open symbols) on the ZrO₂ content of the WC/ZrO₂ nanocomposites. These values, which are summarized in **Table 1**, were estimated from the measured densities and the constant parameters of the nondestructive testing apparatus. Increasing the soft ZrO₂ against the hard brittle phase of WC phase in the composites is greatly improve the ductility of the composites, indicated by a monotonical increasing in the values of Poisson's ratio to achieve a maximum value of 0.268 for the composite with 20% ZrO₂. Compare this value with that one for pure WC (0.004) [14]; one can say that the addition of ZrO₂ improves the ductile characteristics of the fabricated nanocomposite materials. The Young's modulus of the consolidated WC/ZrO₂ nanocomposites is strongly influenced by increasing the ZrO₂ that lead to a linear decreasing in the values of Young's modulus to reach a minimum of 583.2 GPa for WC-20% ZrO₂. This monotonical decrease is attributed to the decreasing of the volume fraction of the hard WC phase.

4. Conclusions

We have employed high-energy ball milling technique to fabricate nanocomposite WC/ZrO₂ powders up to 20 vol.% of ZrO₂. The powders that were milled for 360 ks were consolidated at 1673 K, using SPS technique. The as-consolidated objects have full dense and maintain their nanocrystalline characteristics. The indentation fracture toughness of the composites has been tailored between 7.31 and 19.46 MPa/m^{1/2} by controlling the volume fraction of ZrO₂ matrix between 0.5% to 20%. The results show

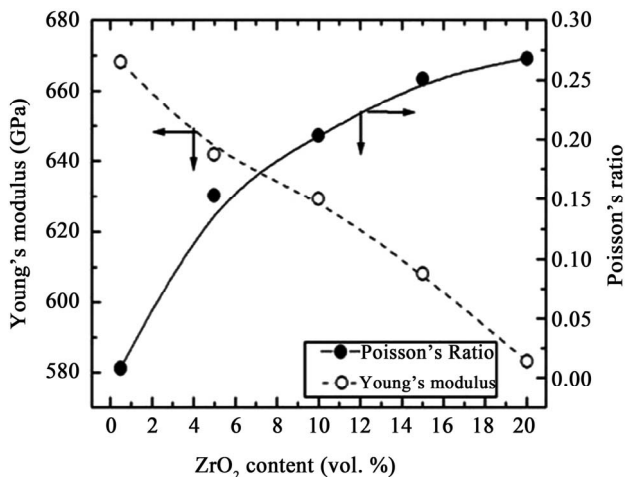


Figure 10. Effect of ZrO₂ content on the Young's modulus (open symbols) and Poisson's ratio (closed symbols) of nanocomposite WC/ZrO₂.

that the Poisson's ratio increased monotonically with increasing the ZrO₂ concentrations to get a maximum value of 0.268 for WC-20 vol.% ZrO₂. High hardness values (20.73 to 22.83 GPa) and Young's modulus (583.2 to 688.2 GPa) were achieved.

5. Acknowledgements

The authors gratefully acknowledge the staff of Mubarak city for scientific research and technology applications (MUCSAT) for funding this work among the internal project of electrochemistry and nanotechnology. Also, the acknowledgement goes to the Egyptian Science and Technology Development Fund (STDF) for funding this work among the STDF project No. 277.

REFERENCES

- [1] M. S. El-Eskandarany, "Mechanical Alloying for Fabrication of Advanced Engineering Materials," William Andrew, New York, 2001, p. 45.
- [2] T. Venkateswaran, D. Sarkar and B. Basu, "Tribological Properties of WC-ZrO₂ Nanocomposites," *Journal of the American Ceramic Society*, Vol. 88, No. 3, 2005, pp. 691-697. [doi:10.1111/j.1551-2916.2005.00129.x](https://doi.org/10.1111/j.1551-2916.2005.00129.x)
- [3] M. S. El-Eskandarany, "Fabrication of Nanocrystalline WC and Nanocomposite WC-MgO Refractory Materials at Room Temperature," *Journal of Alloys and Compounds*, Vol. 296, No. 1-2, 2000, pp. 175-182. [doi:10.1016/S0925-8388\(99\)00508-3](https://doi.org/10.1016/S0925-8388(99)00508-3)
- [4] M. S. El-Eskandarany, A. A. Mahday, H. A. Ahmed and A. H. Amer, "Synthesis and Characterizations of Ball-Milled Nanocrystalline WC and Nanocomposite WC-Co Powders and Subsequent Consolidations," *Journal of Alloys and Compounds*, Vol. 312, No. 1-2, 2000, pp. 315-325. [doi:10.1016/S0925-8388\(00\)01155-5](https://doi.org/10.1016/S0925-8388(00)01155-5)
- [5] H.-C. Kim, I.-J. Shon, J.-K. Yoon and J.-M. Doh, "Consolidation of Ultra Fine WC and WC-Co Hard Materials by Pulsed Current Activated Sintering and Its Mechanical Properties," *International Journal of Refractory Metals & Hard Materials*, Vol. 25, No. 1, 2007, pp. 46-52. [doi:10.1016/j.ijrmhm.2005.11.004](https://doi.org/10.1016/j.ijrmhm.2005.11.004)
- [6] M. Sherif El-Eskandarany, M. Omori, T. Hirai, T. J. Konno, K. Sumiyama and K. Suzuki, "Synthesizing of Nanocomposite WC/MgO powders by Mechanical Solid-State Reduction and Subsequent Plasma-Activated Sintering," *Metallurgical and Materials Transactions A*, Vol. 32, No. 1, 2001, pp. 157-164. [doi:10.1007/s11661-001-0111-0](https://doi.org/10.1007/s11661-001-0111-0)
- [7] B. Basu, T. Venkateswaran and D. Sakar, "Pressureless Sintering and Tribological Properties of WC-ZrO₂ Composites," *Journal of the European Ceramic Society*, Vol. 25, No. 9, 2005, pp. 1603-1610. [doi:10.1016/j.jeurceramsoc.2004.05.021](https://doi.org/10.1016/j.jeurceramsoc.2004.05.021)
- [8] M. S. El-Eskandarany, "Fabrication and Characterizations of New Nanocomposite WC/Al₂O₃ Materials by Room Temperature Ball Milling and Subsequent Consolidation," *Journal of Alloys and Compounds*, Vol. 391, No. 1-2, 2005, pp. 228-235. [doi:10.1016/j.jallcom.2004.08.064](https://doi.org/10.1016/j.jallcom.2004.08.064)
- [9] M. S. El-Eskandarany, M. Omori and A. Inoue, "Solid-State Synthesis of New Glassy Co₆₅Ti₂₀W₁₅ Alloy Powders and Subsequent Densification into a Fully Dense Bulk Glass," *Journal of Materials Research*, Vol. 20, No. 10, 2005, pp. 2845-2853. [doi:10.1557/JMR.2005.0344](https://doi.org/10.1557/JMR.2005.0344)
- [10] G. R. Anstis, P. Chantikul, B. R. Lawn and D. B. Marshall, "A Critical Evaluation of Indentation Techniques for Measuring Fracture Toughness: I, Direct Crack Measurements," *Journal of the American Ceramic Society*, Vol. 64, No. 9, 1981, pp. 533-538. [doi:10.1111/j.1151-2916.1981.tb10320.x](https://doi.org/10.1111/j.1151-2916.1981.tb10320.x)
- [11] B. Basu, J. Vleugels and O. Van-der Biest, "Processing and Mechanical Properties of ZrO₂-TiB₂ Composites," *Journal of the European Ceramic Society*, Vol. 25, No. 16, 2005, pp. 3629-3637. [doi:10.1016/j.jeurceramsoc.2004.09.017](https://doi.org/10.1016/j.jeurceramsoc.2004.09.017)
- [12] H. Miyazaki, Yu-ichi Yoshizawa and K. Hirao, "Effect of the Volume Ratio of Zirconia and Alumina on the Mechanical Properties of Fibrous Zirconia/Alumina Bi-Phase Composites Prepared by Co-Extrusion," *Journal of European Ceramic Society*, Vol. 26, No. 16, 2006, pp. 3539-3546.
- [13] R. C. Garvie, R. H. Hannink and R. T. Pascoe, "Ceramic steel?" *Nature*, Vol. 258, No. 5537, 1975, pp. 703-704. [doi:10.1038/258703a0](https://doi.org/10.1038/258703a0)
- [14] M. S. El-Eskandarany, M. Omori, M. Ishikuro, T. J. Konno, K. Takada, K. Sumiyama, T. Hirai and K. Suzuki, "Synthesis of Full-Density Nanocrystalline Tungsten Carbide by Reduction of Tungstic Oxide at Room Temperature," *Metallurgical and Materials Transactions A*, Vol. 27A, No. 12, 1996, pp. 4210-4213. [doi:10.1007/BF02595669](https://doi.org/10.1007/BF02595669)